

Polydopamine enhances the photocatalytic performance of BiOBr-loaded 3D-printed monolithic photoreactor by fused deposition modeling

Fengrui Wu^{a, d, 1}, Yan Li^{a, d, 1}, Wenxiu Wu^{b, d}, Zhipeng Zhang^{b, d}, Liangbin Lin^{b, d}, Songwei Yang^{b, d}, Lihong Xu^c, Xinshu Xia^{b, d}, Weiming Zhou^{b, d*}, Changlin Cao^{b, d*}, Liren Xiao^{a, d*}

^a College of Chemistry and Materials Science, Fujian Normal University, Fuzhou 350117, China.

^b College of Environmental and Resource Sciences, Fujian Normal University, Fuzhou 350117, China.

^c College of Materials Science and Engineering, Fujian University of Technology, Fuzhou 350117, China.

^d Engineering Research Center of Polymer Green Recycling of Ministry of Education, Fuzhou 350117, China.

* Corresponding authors: wmzhou@fjnu.edu.cn (W.M. Zhou), caochlin3@fjnu.edu.cn (C.L. Cao), xlr1966@fjnu.edu.cn (L.R. Xiao).

¹ These authors contributed equally to this work.

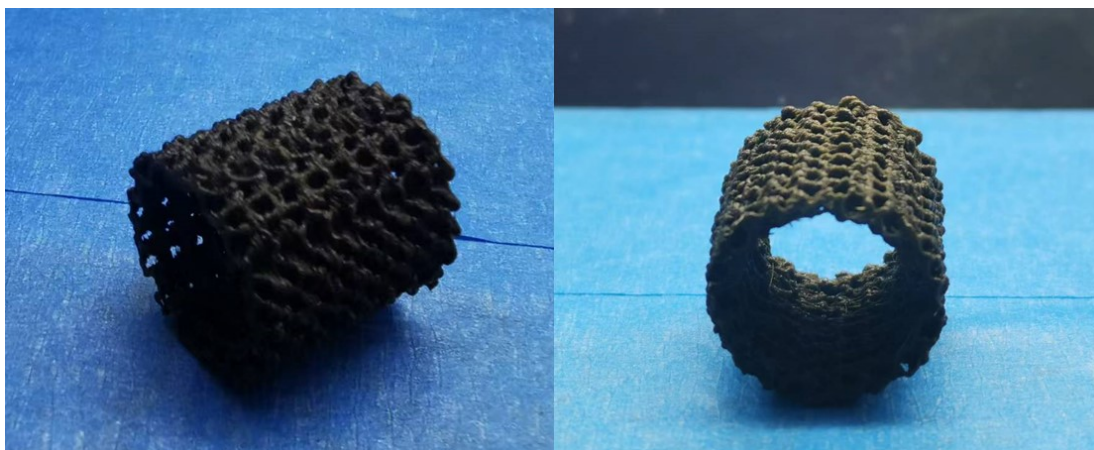


Fig. S1 Digital photos of the 3D-printed monolithic photoreactor, D-type models containing 20 phr of *Chlorella*.

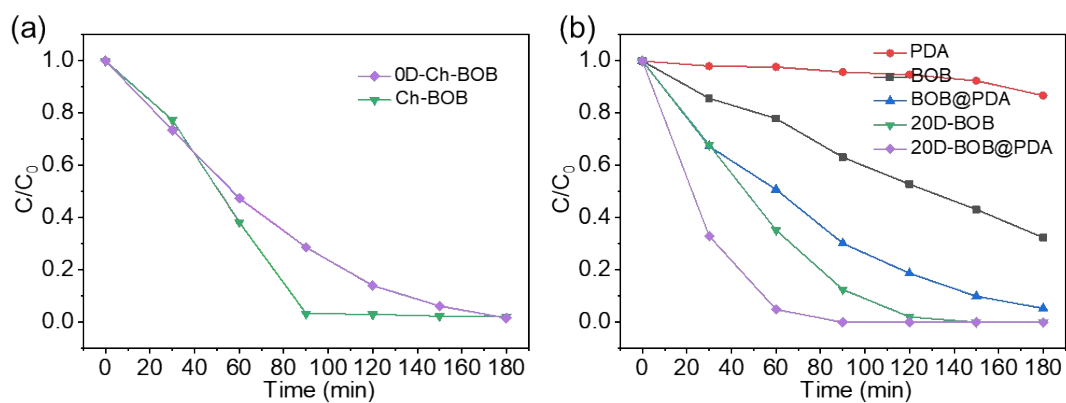


Fig. S2 Photocatalytic degradation curves of as-prepared samples

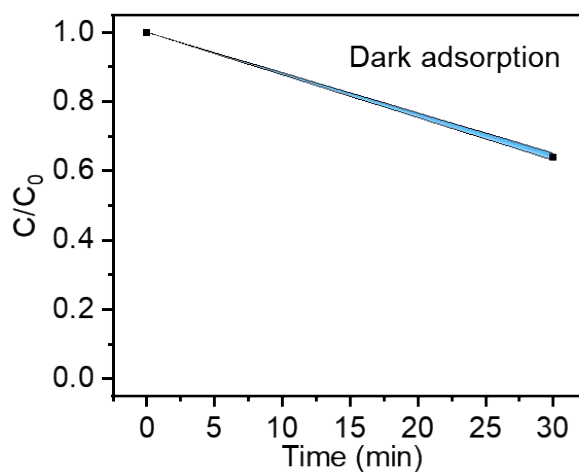


Fig. S3 Dark adsorption curves of 20D-BOB@PDA.

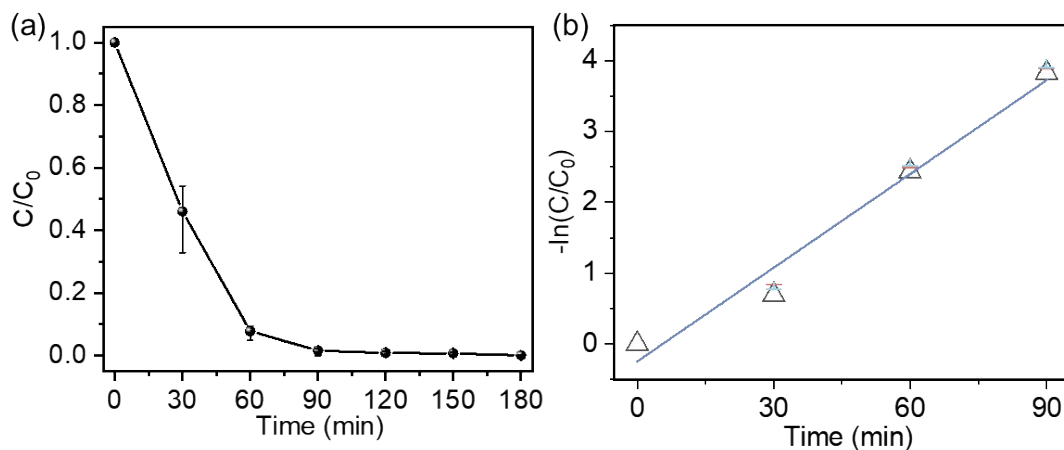


Fig. S4 (a) Photocatalytic degradation curves and (b) equivalent pseudo-first-order kinetic curves of 20D-BOB@PDA for RhB. For all reactions, the error bars represent the standard deviation values obtained from three repeated experiments.

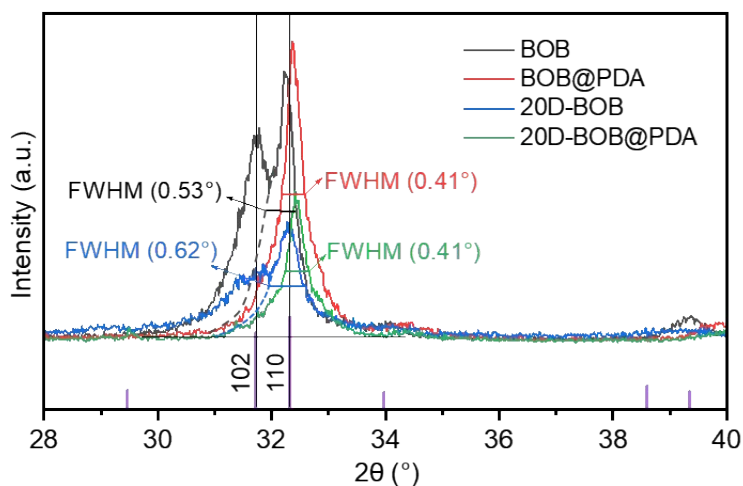


Fig. S5 XRD patterns of BOB, BOB@PDA, 20D-BOB, and 20D-BOB@PDA.

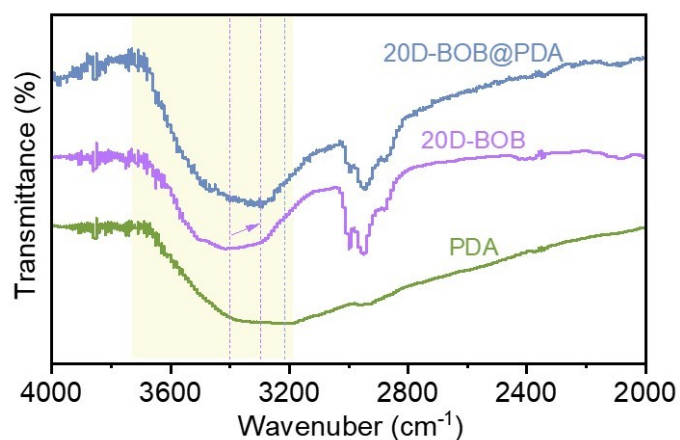


Fig. S6 FT-IR spectra of PDA, 20D-BOB, and 20D-BOB@PDA.

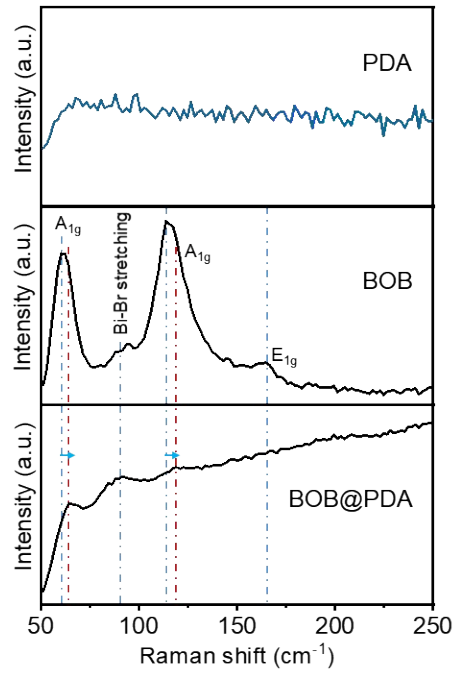


Fig. S7 Raman spectra of BOB, PDA, and BOB@PDA.

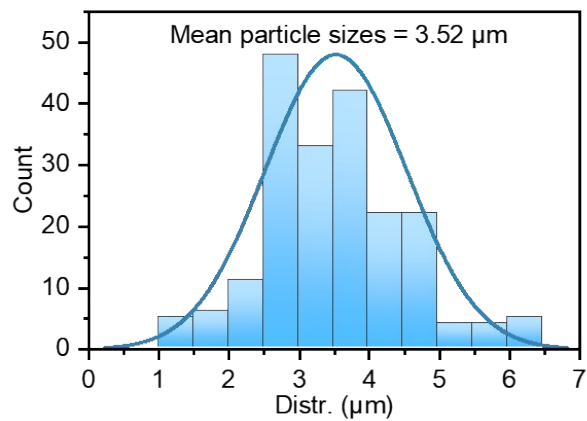


Fig. S8 Particle size distribution of 20D-BOB@PDA.

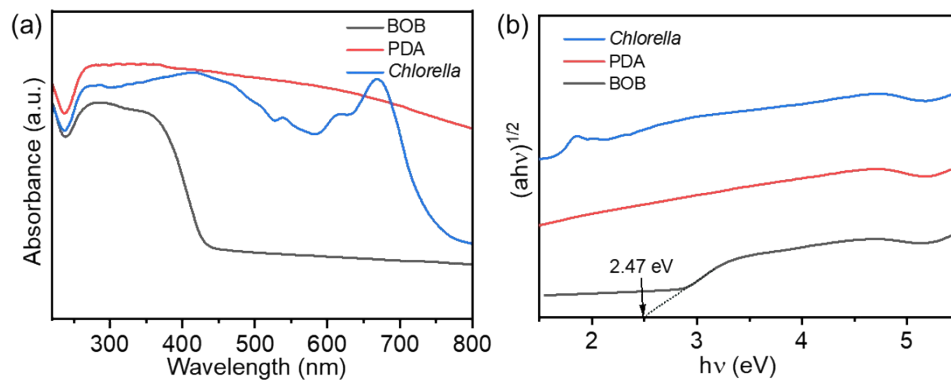


Fig. S9 (a) UV-vis DRS and (b) $(ah\nu)^{1/2}$ versus $h\nu$ curves of BOB, PDA, and *Chlorella*.

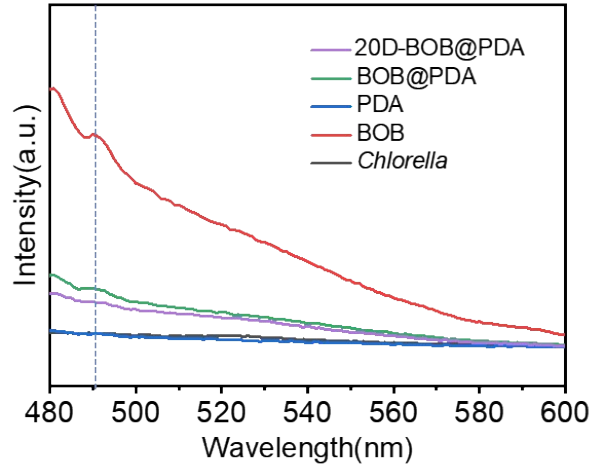


Fig. S10 Photoluminescence spectra of 20D-BOB@PDA, BOB@PDA, PDA, BOB and *Chlorella*.

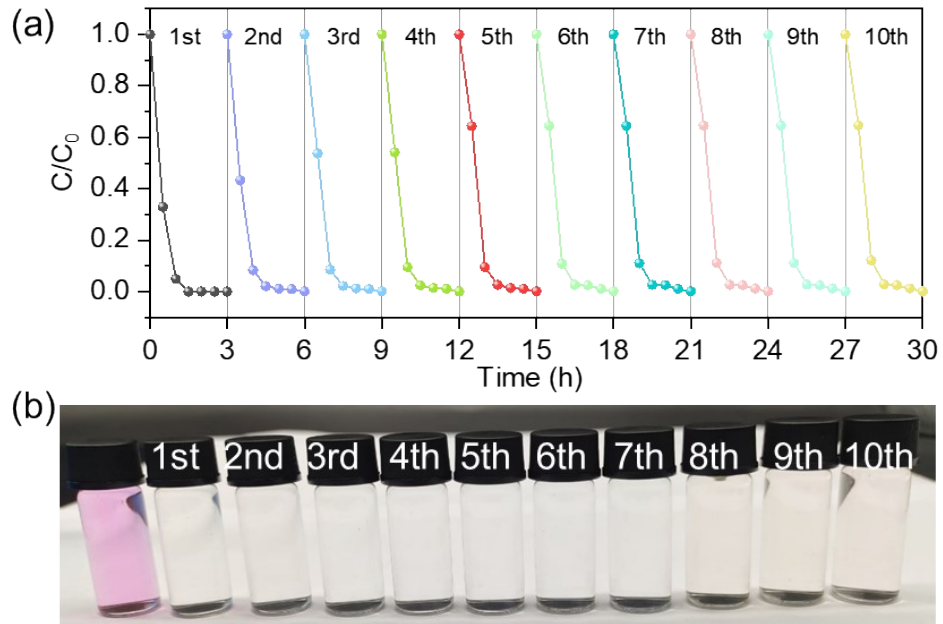


Fig. S11 (a) Photocatalytic degradation curves and (b) digital photo of 20D-BOB@PDA with 10 discontinuous cycles.

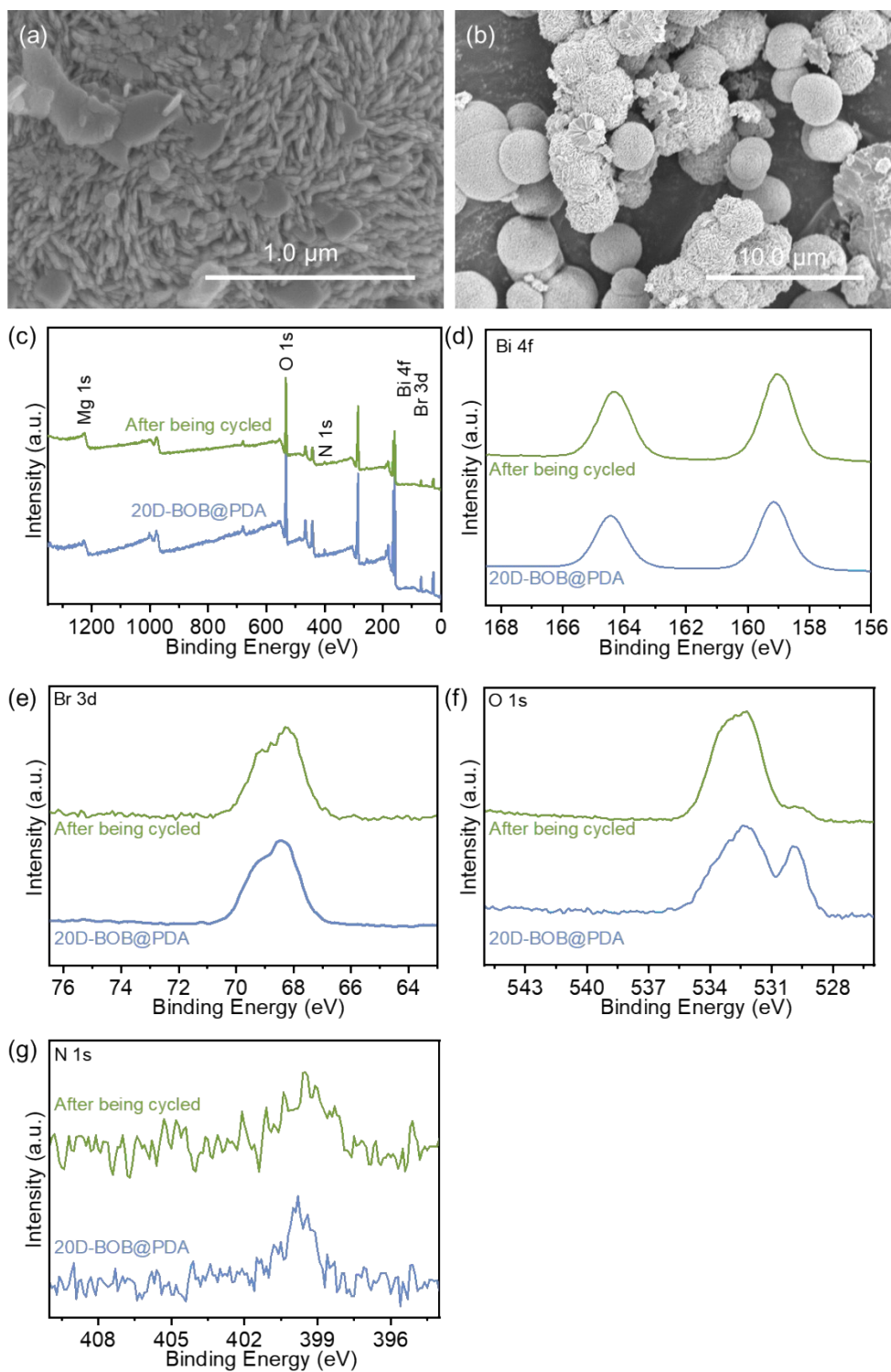


Fig. S12 (a, b) SEM image, (c) XPS survey spectra, and high-resolution XPS spectra for (d) Bi 4f, (e) Br 3d, (f) O 1s, and (g) N 1s of 20D-BOB@PDA and its cycled samples.

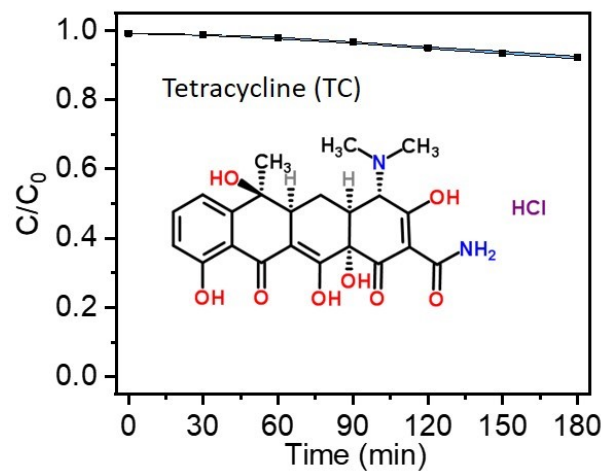


Fig. S13 Photocatalytic degradation curves of TC without catalyst under the same conditions, inset: the molecular structure of TC.

Table S1 The measured loading values of 20D-BOB@PDA

No.	Initial weight (20D, g)	Final weight (20D-BOB@PDA, g)	Weight difference (g)	Load capacity (%)
1	1.2813	1.3037	0.0224	1.75
2	1.2542	1.2777	0.0235	1.87
3	1.2034	1.2246	0.0212	1.76
4	1.2131	1.2353	0.0222	1.83

Table S2 Summaries of crystal information for (110) crystal planes

Samples	FWHM (°)	Bragg's angle (2θ, °)	Crystal size (D, nm)
BOB	0.53	32.22	15.60
BOB@PDA	0.41	32.41	20.17
20D-BOB	0.62	32.28	13.35
20D-BOB@PAD	0.41	32.41	20.17

The crystal size (D) of the samples was calculated using Scherrer equation ¹ :

$$D = \frac{0.9\lambda}{\beta \cos \theta}$$

where λ is the X-ray wavelength (Cu K α , $\lambda=1.54056\text{\AA}=0.154056\text{nm}$), β is the corrected full width at half maximum (FWHM), and θ is the Bragg's angle.

Reference

- 1.C. Rodwihok, K. Charoensri, D. Wongratanaphisan, W. M. Choi, S. H. Hur, H. J. Park and J. S. Chung, *Journal of Materials Science & Technology*, 2021, **76**, 1-10.